Magnetic structure and spin reorientation of the Mn ions in NdMnO3

S. Y. Wu, C. M. Kuo, H. Y. Wang, W.-H. Li, K. C. Lee et al.

Citation: J. Appl. Phys. **87**, 5822 (2000); doi: 10.1063/1.372534
View online: http://dx.doi.org/10.1063/1.372534
View Table of Contents: http://jap.aip.org/resource/1/JAPIAU/v87/i9
Published by the American Institute of Physics.

Related Articles

Magnetic transitions in erbium at high pressures
J. Appl. Phys. 111, 07E104 (2012)

Twin-Foucault imaging method
Appl. Phys. Lett. 100, 061901 (2012)

Phase instability of magnetic ground state in antiperovskite Mn3ZnN: Giant magnetovolume effects related to magnetic structure
J. Appl. Phys. 111, 07A904 (2012)

Magnetodielectric effect in Z-type hexaferrite
Appl. Phys. Lett. 100, 032901 (2012)

Confinement effects on the low temperature magnetic structure of MnP nanocrystals
Appl. Phys. Lett. 99, 182506 (2011)

Additional information on J. Appl. Phys.

Journal Homepage: http://jap.aip.org/
Journal Information: http://jap.aip.org/about/about_the_journal
Top downloads: http://jap.aip.org/features/most_downloaded
Information for Authors: http://jap.aip.org/authors

ADVERTISEMENT

Downloaded 12 Feb 2012 to 140.112.24.214. Redistribution subject to AIP license or copyright; see http://jap.aip.org/about/rights_and_permissions

Magnetic structure and spin reorientation of the Mn ions in $NdMnO_3$

S. Y. Wu, C. M. Kuo, H. Y. Wang, W.-H. Li,[a] and K. C. Lee
Department of Physics, National Central University, Chung-Li, Taiwan 32054

J. W. Lynn
NIST Center for Neutron Research, NIST, Gaithersburg, Maryland 20899

R. S. Liu
Department of Chemistry, National Taiwan University, Taipei, Taiwan 106

The crystal structure and magnetic ordering of the Mn spins in polycrystalline $NdMnO_3$ have been investigated by means of neutron diffraction and ac magnetic susceptibility measurements. The compound crystallizes into an orthorhombic symmetry of space group *Pbnm*. Three peaks were observed in the temperature dependence of the in-phase component of the ac susceptibility, $\chi'(T)$. Neutron diffraction measurements show that all three peaks observed in $\chi'(T)$ are of magnetic origin, and are associated with the ordering and the reorientation of the Mn spins. Both ferromagnetic and antiferromagnetic couplings between the Mn spins were observed, resulting in a noncollinear magnetic structure. The Mn spins order at $T_m \approx 75$ K, and the moment saturates at ~20 K at $\langle \mu_z \rangle = 2.21\ \mu_B$. © *2000 American Institute of Physics.* [S0021-8979(00)62308-3]

Although double exchange (DE) interactions[1] may be used to explain the simultaneous observation of itinerant electron behavior and ferromagnetism in the hole doped perovskite-type manganites $R_{1-x}A_xMnO_3$ (*R*=rare-earth ions and *A*=alkaline-earth ions), the overall lattice symmetry and local lattice distortions need to be considered as well in understanding the novel properties of these systems. Apparently, the hole carrier density and the overlap between the manganese and oxygen orbitals are the two major parameters that govern the transport and magnetic properties of the systems. The former can be controlled by partially replacing the trivalent lanthanide with a divalent alkaline earth, that introduces holes into the e_g orbitals. The latter can be modified by changing the average ionic size of the cations, and thereby adjusting the e_g-electron transfer interaction.[2] Generally, using a smaller rare-earth ion produces a larger lattice distortion of the pervoskite structure, which results in a smaller Mn–O–Mn bond angle and a narrower e_g-electron bandwidth. This then reduces the degree of hybridization between the Mn *3d* e_g and O *2p* σ orbitals and weakens the strength of DE interaction. Compared to the most intensely investigated La-based system, the strength of DE interactions in the Nd-based system is weaker[3] since a larger lattice distortion is achieved by the smaller Nd ions. This results in a closer competition between the DE interaction, and the electron–phonon interaction, and electron–electron Coulomb interaction in $Nd_{1-x}Ca_xMnO_3$.[4,5] In this paper we present the magnetic structure of the Mn ions in $NdMnO_3$, studied using ac magnetic susceptibility and neutron diffraction measurements.

Polycrystalline $NdMnO_3$ was prepared by the standard solid-state reaction technique. The compound was characterized by a complete structural analysis using high-resolution neutron powder diffraction. The data were collected on BT-1, the 32-detector powder diffractometer at the NIST Center for Neutron Research, employing neutrons of wavelength 1.5401 Å and angular collimations of 15′-20′-7′ full width at half maximum (FWHM) acceptance. Crystal structure analysis was performed using the GSAS program[6] of Larson and Von Dreele, following the Rietveld method.[7] The refinements were carried out assuming the symmetry of orthorhombic space group *Pbnm*. There are no unexpected peaks at present, showing that the sample is essentially single phase. Careful analysis of the occupancy factors shows that both the Nd and O sites are almost fully occupied, and the chemical composition that we obtained for the compound is $NdMnO_{2.997}$. We estimated that the impurity level is less than 3%. The structure may be viewed as a stacking of MnO_2–NdO layers (*a*-*b* planes) along the *c* axis direction.

ac magnetic susceptibility was then measured to search for magnetic transitions. The data were collected using a weak driving field of frequency 100 Hz and rms (root-mean-square) strength 1 Oe, with and without an applied dc field. Both the in-phase component χ' and the out-of-phase component χ'' were measured. Shown in Fig. 1 are the variations of χ' with temperature under various applied fields. The main feature seen is the sharp peak at ~75 K. This peak is associated with the ordering of the Mn spins, and it has an antiferromagnetic character as its amplitude decreases and peak position shifts to a lower temperature when a dc field is applied. The paramagnetic portion of χ', however, shows a ferromagnetic character, as it displays a Curie–Weiss behavior as for a ferromagnetic system, $\chi'(T) = \chi'_0 + C/(T-\theta)$ with θ positive. The solid curve shown in the high temperature portion of Fig. 1 is an extrapolation of a fit to the χ' data obtained between 120 and 325 K (not shown) to the above expression with fitted θ=85 K and effective moment $\mu_{\text{eff}} = 2.03(5)\ \mu_B$. At lower temperatures, two small but definite peaks with maxima at 44 and 14 K are also clearly seen. The former is associated with the change of the canting angle of the Mn moment (see below), and this behavior is much

[a]Electronic mail: whli@joule.phy.ncu.edu.tw

 © 2000 American Institute of Physics

Downloaded 12 Feb 2012 to 140.112.24.214. Redistribution subject to AIP license or copyright; see http://jap.aip.org/about/rights_and_permissions

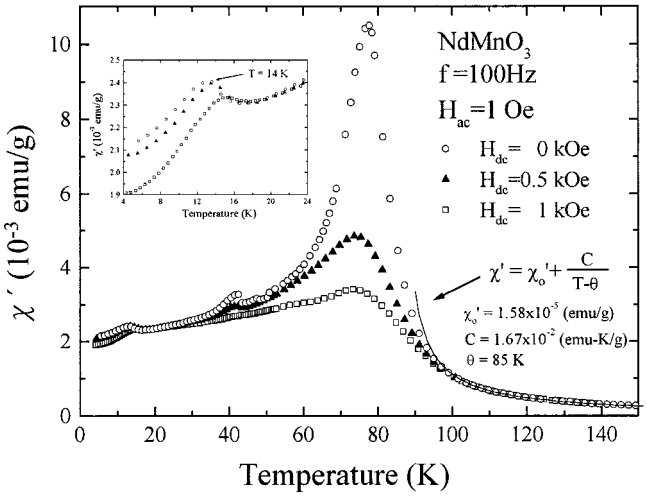

FIG. 1. Temperature dependence of χ' measured using a weak driving field without and with an applied dc field. Three definite peaks at 75, 44, and 14 K are clearly evident.

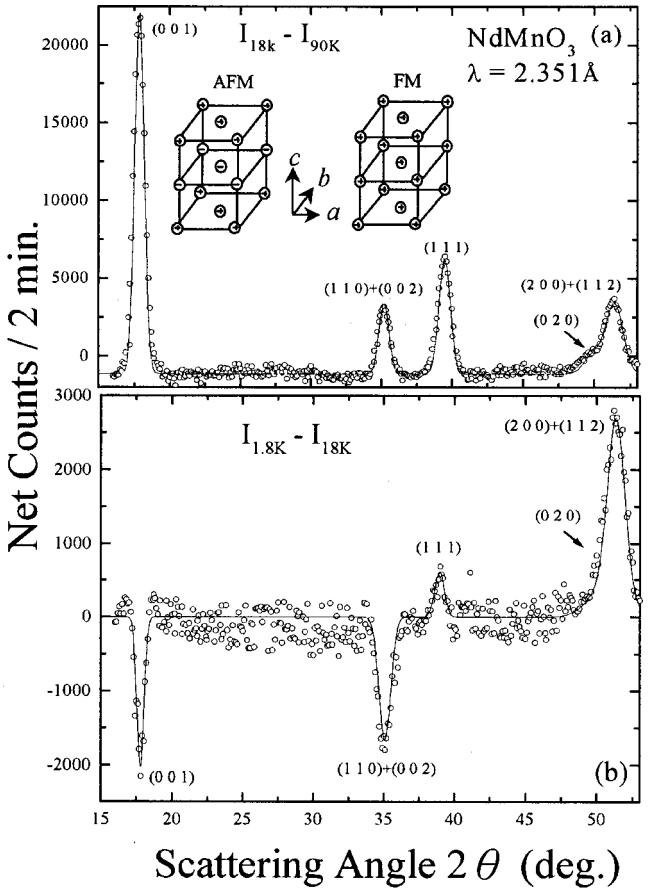

FIG. 2. Difference patterns observed (a) between 18 and 90 K and (b) between 1.8 and 18 K. The solid curves are fits of the data to the Gaussian instrumental resolution functions. The inset in (a) shows schematic representation of the AFM and FM components, where the plus and minus signs denote that the moments point along opposite directions.

reduced as a dc field is applied. The 14 K transition corresponds to the reorientation of the Mn spin (see below), which is still clearly evident at an applied dc field of 1 kOe, as can be seen in the inset of Fig. 1. No ac losses were detected, as essentially zero values were obtained for χ'' at all temperatures studied.

Neutron diffraction was performed to explore the spin structures of the Mn ions. The measurements were carried out at NIST, and the data were collected on the BT-2 triple-axis spectrometer operated in double-axis mode, using a conventional setup with pyrolytic graphite monochromator and filter. Neutrons of wavelength 2.351 Å and angular collimations of 60′-40′-40′ FWHM acceptance were used. The magnetic signal was identified using the standard subtraction technique.[8] In Fig. 2 we show two difference patterns thus obtained, where the indices marked are based on the nuclear unit cell. The peaks shown in Fig. 2(a) are the peaks that develop as the temperature is reduced from 90 to 18 K, and signify Mn spin ordering. These magnetic peaks may be grouped into two types that belong to two separate Fourier components. One has the nearest-neighbor Mn spins aligned parallel in the *a-b* planes but antiparallel along the *c* axis direction, hence a spin structure consisting of ferromagnetic sheets coupled antiferromagnetically, as the one marked as AFM shown in the inset of Fig. 2(a). This component gives rise to the {001} and {111} magnetic peaks, and will be referred to as the AFM component of the spin structure. The second component has the Mn spins aligned parallel along all three crystallographic directions, hence a simple ferromagnetic structure, as the one marked as FM shown in the inset of Fig. 2(a). This component will be referred to as the FM component of the spin structure, which produces the {110}+{002}, {020}, and {200}+{112} magnetic reflections.

The difference pattern shown in Fig. 2(b) clearly indicates that as the temperature is reduced from 18 to 1.8 K the intensities of the AFM{001} and FM{110}+{002} reflections decrease, while that of the AFM{111} and FM{200}+{112} reflections increase. This behavior is associated with a reorientation of the Mn spins. Figure 3 shows the temperature dependence of the intensities of representative magnetic peaks. There are several points to note about the order-parameter measurements shown in Fig. 3: (1) The intensity scales used in the two plots are different by a factor of about 4, with the AFM intensity being the stronger. (2) The ordering temperature of the Mn spins, as determined by the inflection point of the AFM{001} data, is $T_m \approx 75$ K. This is the same temperature at which the most pronounced peak in $\chi'(T)$ occurs. (3) On reducing the temperature the AFM{001} intensity increasing monotonically, and it reaches the maximum at ~20 K, where a plateau also appears in the FM{200}+{112} data. At this temperature the Mn moment saturates. (4) Below 14 K, the AFM{001} intensity decrease with decreasing temperature. Shown as an inset in Fig. 3(a) is a re-plot of the low temperature data, so that these two sets of data can be compared directly. The data clearly show that the downturn in the AFM{001} intensity is accompanied by the further increase of the FM{200}+{112} intensity. These changes mark the onset of the reorientation of the Mn spins, which is completed at ~4 K. We note that a corresponding peak, which is only weakly affected by an applied ac field, also appears in $\chi'(T)$. (5) Around 40 K, a plateau is seen in the FM{200}+{112} data. Correspondingly, a weak peak ap-

Downloaded 12 Feb 2012 to 140.112.24.214. Redistribution subject to AIP license or copyright; see http://jap.aip.org/about/rights_and_permissions

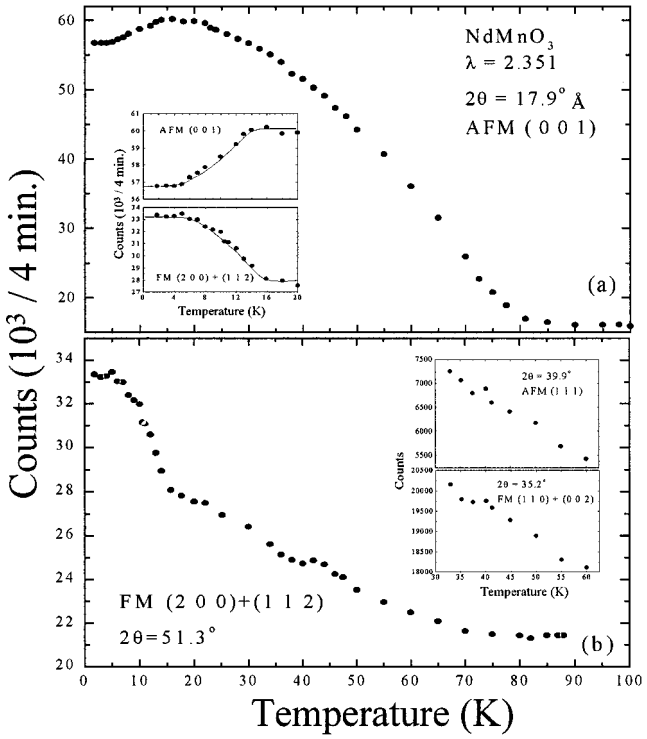

FIG. 3. Variations of the magnetic intensities with temperature for four representative peaks. The inset in (a) is a replot of the low temperature portions of the AFM{001} and FM{112}+{200} intensities, such that they can be compared directly. Plateaus in the vicinity of 40 K are evident in the AFM{111} and FM{110}+{002} integrated intensities shown in the inset of (b).

pears in $\chi'(T)$ as well. Although no obvious anomaly is seen in the AFM{001} data, anomalies are nevertheless present in the AFM{111} and FM{110}+{002} data plotted in the inset of Fig. 3(b), where the temperature dependence of the AFM{111} and FM{110}+{002} integrated intensities in the vicinity of $T=40$K are shown. Both plots reveal a plateau around 40 K. The intensity ratios between the AFM and the FM components are then different below and above this temperature regime, showing a change in the direction of the Mn moments has occurred.

If we make the physically reasonable assumption that the magnitude of the moment on each Mn ion is the same, then the two spin directions corresponding to the AFM and the FM components must be perpendicular. A superposition of these two components results in a noncollinear magnetic structure for the Mn spins. Denoting α (β) as the angle between the AFM (FM) moment and the *c* axis, employing the intensity formula[9] for noncollinear structure and using the angles α and β as fitting parameters, we went through 36×36 model calculations allowing α or β to change by 5° for each calculation. The spin configuration that best fits the patterns observed at 18 K have $\alpha=90°$ and $\beta=15°$, or $\alpha=75°$ and $\beta=45°$ at 1.8 K. Unfortunately, the specific moment direction in the *a*-*b* plane cannot be determined from our powder data due to the similarity between the *a* and *b* axes. Shown in Fig. 4 are the proposed structure for the AFM

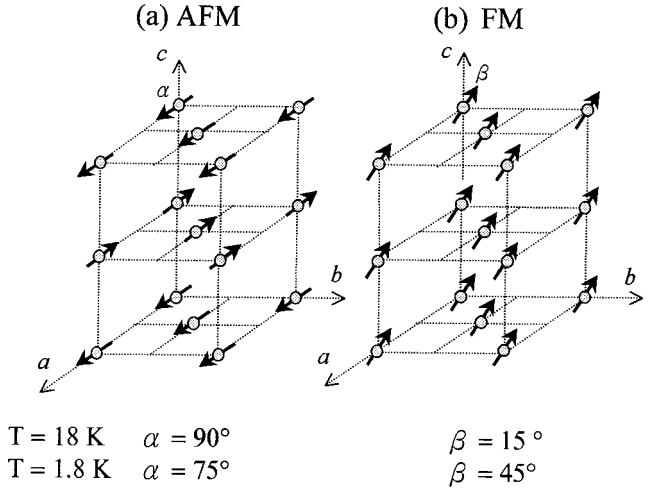

FIG. 4. Proposed magnetic structure for the Mn ions.

and FM components, where the former is arbitrary chosen to lie in the *a*-*c* plane, hence the latter lies in the *b*-*c* plane, for clarity of presentation. Spin configurations obtained by rotation of the structures shown in Fig. 4 about the *c* axis through a finite angle fit equally well to our data. We estimated that the uncertainty in the direction of the out-of-plane moment is about $\pm5°$, whereas that of the in-plane moment cannot be resolved using our powder data. This structure observed for the Mn spins in $NdMnO_3$ is similar to what has been reported for the La-based and Pr-based compounds.[10–12] The low temperature saturated moment that we obtained was $\langle\mu_z\rangle = 2.21(5)\mu_B$. We finally remark that no evidence of the Nd ordering was seen down to 1.8 K. A lower temperature may be needed before the effects due to the Nd ordering become significant. This issue was not considered in the present analysis.

The work at NCU was supported by the NSC of R.O.C. under Grant NO. NSC 88-2112-M-008-002.

[1] C. Zener, Phys. Rev. **82**, 403 (1951).
[2] H. Y. Hwang, S.-W. Cheong, P. G. Radaelli, M. Marezio, and B. Batlogg, Phys. Rev. Lett. **75**, 914 (1995).
[3] V. Caignaert, F. Millange, M. Hervieu, E. Suard, and B. Raveau, Solid State Commun. **99**, 173 (1996).
[4] K. Liu, X. W. Wu, K. H. Ahn, T. Sulchek, C. L. Chien, and J. Q. Xiao, Phys. Rev. B **54**, 3007 (1996).
[5] M. Tokunaga, N. Miura, Y. Tomioka, and Y. Tokura, Phys. Rev. B **57**, 5259 (1998).
[6] A. C. Larson and R. B. Von Dreele, LANL Report LA-UR-86-748, LANL, Los Alamos, NM 87545 (1990).
[7] H. M. Rietveld, J. Appl. Crystallogr. **2**, 65 (1969).
[8] H. Zhang, J. W. Lynn, W.-H. Li, and T. W. Clinton, Phys. Rev. B **41**, 11229 (1990).
[9] G. L. Squires, *Introduction to the Theory of Thermal Neutron Scattering* (Cambridge Univ. Press, Cambridge, 1976).
[10] V. A. Cherepanov, Y. L. Barkhatova, A. N. Petrov, and V. I. Voronin, J. Solid State Chem. **118**, 53 (1995).
[11] C. Ritter, M. R. Ibarra, J. M. De Teresa, P. A. Algarabel, C. Marquina, J. Blasco, J. Gareia, S. Oseroff, and S.-W. Cheong, Phys. Rev. B **56**, 8902 (1997).
[12] Q. Huang, A. Santoro, J. W. Lynn, R. W. Erwin, J. A. Borchers, J. L. Peng, and G. L. Greene, Phys. Rev. B **55**, 14987 (1997).

Downloaded 12 Feb 2012 to 140.112.24.214. Redistribution subject to AIP license or copyright; see http://jap.aip.org/about/rights_and_permissions